Inkjet Printing of Conductive Inks with High Lateral Resolution on Omniphobic "R F Paper" for Paper-Based Electronics and MEMS

WILEY-VCH

DOI: 10.1002/XXXXX
Article type: Communication

Inkjet Printing of Conductive Inks with High Lateral Resolution on Omniphobic "R^F Paper" for Paper-Based Electronics and MEMS

Joshua Lessing[1], Ana C. Glavan[1], S. Brett Walker[2,3], Christoph Keplinger[1], Jennifer A. Lewis[2,3,] and George M. Whitesides[1,2,*]*

[* corresponding authors] Prof. J. A. Lewis and Prof. G. M. Whitesides
E-mail: jalewis@seas.harvard.edu and gwhitesides@gmwgroup.harvard.edu

Prof. G. M. Whitesides
[1] Department of Chemistry and Chemical Biology, Harvard University, 12 Oxford Street, Cambridge, MA 02138, (USA).
[2] Wyss Institute for Biologically Inspired Engineering, Harvard University, 3 Blackfan Circle, Boston, MA 02115, (USA)

Dr. J. Lessing, A.C. Glavan, Dr. C. Keplinger
[1]Department of Chemistry and Chemical Biology, Harvard University, 12 Oxford Street, Cambridge, MA 02138, (USA)

Dr. S. B. Walker, Prof. J. A. Lewis
[2] Wyss Institute for Biologically Inspired Engineering, Harvard University, 3 Blackfan Circle, Boston, MA 02115, (USA)
[3]Harvard School of Engineering and Applied Sciences, 29 Oxford Street, Cambridge, MA 02138, (USA)

Keywords: inkjet printing, omniphobic paper, electroadhesion, MEMS, electrochemistry

Main Text

This paper describes the use of omniphobic "fluoroalkylated paper" ("R^F paper")[1] as a substrate for inkjet printing of aqueous inks that are the precursors of electrically conductive patterns. By controlling the surface chemistry of the paper, it is possible to print, with high resolution, conductive patterns that remain conductive after folding and exposure to common solvents. Inkjet printing on omniphobic paper is a promising method of fabrication for low-cost, flexible, foldable, and disposable conductors on paper (and other flexible substrates) for electronics, microelectromechanical systems (MEMS), displays, and other applications. The ability to resist wetting by liquids with a wide range of surface tensions, combined with foldability, mechanical flexibility, light weight, low cost, and gas permeability, makes omniphobic R^F paper a versatile alternative to the polymer, glass and silicon-based materials upon which printed electronics are currently being deposited.

To make printing the primary platform for patterning flexible conductors, inexpensive functional inks and substrates must be developed and integrated with a fabrication process capable of broad use. Paper, which is both ubiquitous and inexpensive, has been used as a substrate for printed electronics since the 1960s, when Brody and Page at Westinghouse Electric first stencil-printed inorganic thin-film transistors on paper.[2, 3] Despite many advances in the field, [4-9] conventional cellulose-based paper still remains an underutilized substrate in commercial applications other than conventional printing,[10, 11] due, in part, to the poor barrier properties it provides for liquids. Wetting has the effect of dispersing inks deposited on the substrate, and lowering the resolution and conductivity of printed structures. Moreover, since paper is

hygroscopic, changes in ambient humidity can alter the performance of the printed circuit.

Common methods for printing electronics on paper (e.g., gravure, screen printing, stencil printing, chemical vapor deposition with shadow masking) [10, 12] require the creation of a master (a custom-patterned component such as a screen, stencil, or mask) for printing each new pattern. The fabrication of these masters is a time-consuming and often expensive process, which is incompatible with rapid prototyping and mass customization of electronics, although these technologies are widely used in large-scale manufacturing. Russo et al. have recently developed a pen-on-paper approach for fabricating electronic structures on paper,[13] but the resolution of this method is limited to a few hundred microns or higher.

Here, we report a method for high-resolution printing of conductive patterns on paper that both advances the use of paper substrates for printed electronics, and contributes to our program on low-cost, paper-based diagnostics.[14-26] The major innovation in this work is the use of omniphobic paper[1] as a substrate for the deposition of multiple inks using a piezoelectric inkjet printer. Piezoelectric inkjet printing is a non-contact, additive, and high-precision printing method (with resolution typically ≥ 20 μm, though higher resolution has been obtained at the laboratory scale[10, 27, 28]), that does not require the generation of a master, but instead creates patterns based on easily modifiable digital files.[10, 29] The precise control over the positioning of the droplets and over the interfacial free energy of the paper substrate enabled us to print, with high resolution, conductive patterns that are resistant to damage from exposure to common solvents and to folding.

We modified the surface free energy of paper using a fast vapor-phase treatment with organosilanes.[1] This process, which occurs in approximately five minutes, does not require wetting (and distorting) the paper, or removal of solvents. Treatment with non-fluorinated organosilanes renders paper hydrophobic; treatment with highly fluorinated compounds such as fluoroalkyltrichlorosilanes transforms paper into a material that is omniphobic (both hydrophobic and oleophobic).[1] In both cases, the chemical modifications result in engineered papers with mechanical properties independent of humidity; these papers retain the mechanical flexibility and low resistance to gas transport of untreated paper.[1]

We used four commercially available reagents to study the effect of the change in interfacial free energy (provided by the covalently grafted organosilane) on the resolution of printed conductive features: (i) (3,3,4,4,5,5,6,6,7,7,8,8,9,9,10,10,10-heptadecafluorodecyl) trichlorosilane ($CF_3(CF_2)_7CH_2CH_2SiCl_3$, "$C_{10}^F$"), (ii) methyltricholorosilane (CH_3SiCl_3, "C_1^H"), (iii) decyltrichlorosilane ($CH_3(CH_2)_9SiCl_3$, "C_{10}^H"), and (iv) tris(dimethylamino)silane (TDA). A relatively smooth paper, (Canson tracing paper, Model No. 702-321) is used as a substrate for applications requiring maximum lateral resolution; this choice of paper minimizes irregularities in the conductivity and resolution of printed features induced by surface roughness.

We first examined, by means of apparent static (θ_s) contact angle[31] measurements, the wettability of the organosilane-modified paper substrates.[1] In the absence of this treatment, water droplets are found to immediately wick into the paper (**Figure 1**). By contrast, silanization renders the papers hydrophobic, i.e., water no longer wicks into them, but rather forms droplets on their surfaces with apparent static contact angles,

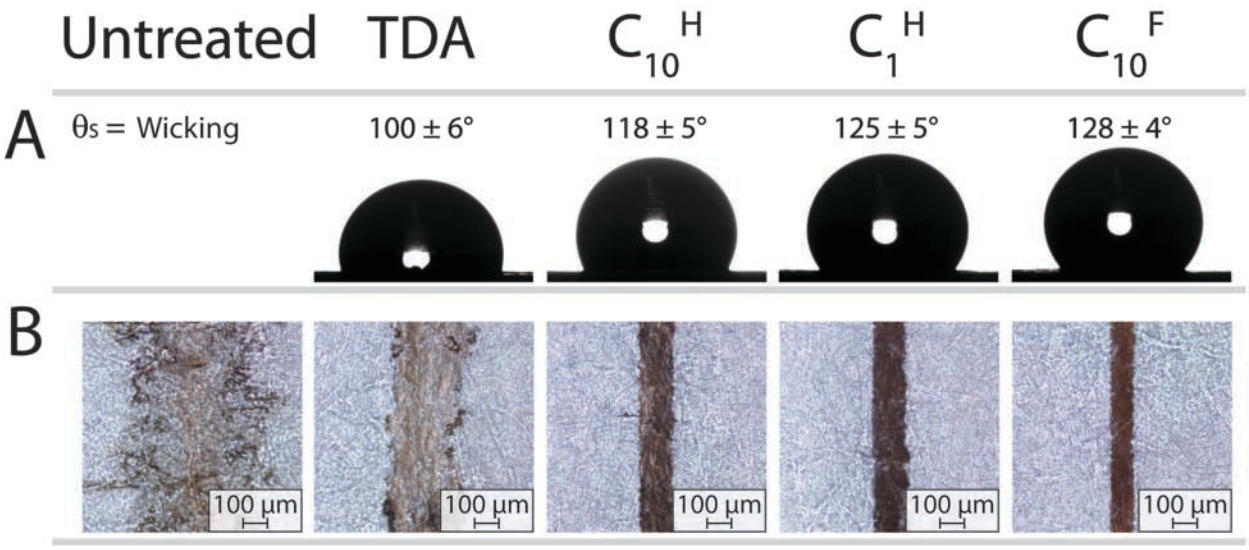

Figure 1: (A) Images of 10-µL drops of water on a series of Canson tracing papers, modified with different organosilanes, and their corresponding static contact angles (Θ_s) (Error bars: standard deviations for *n*=7 measurements). **(B)** Optical micrographs of silver wires printed on the modified or unmodified Canson tracing paper substrates using the reactive silver ink with a target resolution of 80 µm.

θ_s^{H2O}, between 100º ± 6 (for TDA, *n*=7) and 128º± 4 (for C_{10}^F, *n*=7). Based on the static contact angle measurements, the hydrophobicity of the surfaces appears to increase according to the series: untreated paper < TDA < C_{10}^H < C_1^H < C_{10}^F.

Figure 1 clearly demonstrates that the wetting of untreated and silanized paper by water correlates with the lateral resolution of the printed conductive features. Canson tracing paper, untreated or silanized with TDA, C_1^H, C_{10}^H, and C_{10}^F, is used as a substrate for the inkjet printing of 80-μm-wide wires (the intended width based on the features in the digital file) using reactive silver ink dispensed by a Fuji Dimatix DMP-2831 printer (see Supplementary Information for details). We used this reactive silver ink [30] because it yields patterned features whose electrical conductivity is superior to that of features obtained using commercial silver nanoparticle inks. The reactive silver inks are essentially modified Tollens' reagents: that is, aqueous solutions that contain a soluble complex of silver ions and a strong reducing agent—formic acid – present as ammonium formate . The silver ions are reduced to silver particles as the formic acid is generated upon evaporation of the volatile ammonia from a solution of ammonium formate upon printing and subsequent heating at modest temperatures (≤ 120 °C). This process results in patterned features with conductivities that are 60-90% of the bulk conductivity of silver, since there are no polymeric or other organic residues in the ink formulation.[30] Optical micrographs show that the lateral resolution of printed features improves with increasing hydrophobicity: untreated paper = 585 ± 87 μm, TDA = 292 ± 34 μm, C_{10}^H = 149 ± 31 μm, C_1^H = 137 ± 13 μm, and C_{10}^F = 90 ± 5 μm (*n*=10 measurements of the feature width). The lateral resolution of the printed features is linearly correlated with the apparent static contact angle, θ_s^{H2O} on the surface of each paper (**Figure S1**). This effect

is most pronounced for C_{10}^{F}–treated paper, which shows a substantial improvement in maximum lateral resolution compared to the untreated paper substrate. The SEM images reveal that the hydrophobicity of the C_{10}^{H}, C_{1}^{H}, and C_{10}^{F} –treated paper surfaces serves to focus the deposition of silver particles into a smaller area (**Figure S2**), thus enabling printing of continuous conductive features. The resistance of the printed wires decreases with increasing hydrophobicity: R^{TDA} =2371 ± 1618 Ω, R^{C10H} =400 ± 206 Ω, R^{C1H} =265 ± 64 Ω, and R^{C10F} =132 ± 25 Ω (these resistances are measured over a length of 1 cm for n=7 distinct features). The observed conductivity of wires printed on silanized papers stands in contrast with the very high resistance of the features printed on untreated paper (resistance greater than the detection limit of our multimeter ~10 MΩ).

The resolution of inkjet-printed patterns is limited by several factors: the wettability of the substrate, the hydrodynamics of the jetted microdroplets, and the volatility of the constituents of the ink.[29] Typically, 20 μm is considered the smallest feature size achievable via inkjet printing.[33] Features of this size are typically achieved using 1-pL droplets, but can also be achieved by tuning the waveform of 10-pL cartridges to achieve droplet volumes below 10 pL. We chose our most hydrophobic paper in the series, Canson tracing paper treated with C_{10}^{F} (Θ_s^{H2O} = 129°± 4, n=7), to test the maximum lateral resolution achievable using reactive silver ink dispensed from a 10-pL Dimatix cartridge. A 10-pL spherical droplet has a diameter of 27 μm. We printed lines with thickness determined by the width of single drops, with a spacing set at 20 μm between consecutive drops. SEM imaging (**Figure S3**) shows that a maximum lateral resolution of 28 ± 5 μm and a line edge roughness of 6 μm is achieved on this paper. To the best of our knowledge, this resolution has never before been achieved with droplets of this

volume, suggesting that a high level of control over line width can be achieved by decreasing the surface free energy of the substrate. However, while the 28 μm-wide feature appears to be continuous by SEM, it is not conductive. Since its width is on the same size scale as that of the individual cellulose fibers, the surface roughness of the tracing paper likely introduces local discontinuities in the patterned wires. These discontinuities could be remedied simply by printing multiple overlapping layers of ink. Unfortunately, our printer cannot achieve accurate multilayer printing at this scale due to its inability to reproduce droplet location below an accuracy of ±25 μm. We anticipate that printing of microscopic wires (< 30μm) with a 10-pL droplet would be possible by using a printer with higher droplet-positioning accuracy and a paper with lower surface roughness (e.g., nanocellulose paper). [32]

To test the performance of the inkjet-printed silver features upon exposure to common solvents, we quantified the change in electric resistance of silver wires printed on C_{10}^{F} paper after drops of solvent are deposited on their surface. Ten 50-μL drops of solvent are deposited along the path of each silver wire (n=7, 10 cm-long, and 1 mm-wide wires were tested per solvent). We found that the percentage change in resistance after 30 min of solvent exposure is negligible for conventional solvents used for inkjet printing (e.g., water, ethanol, and glycerin). We also tested solvents (toluene, glacial acetic acid, chloroform, dimethyl sulfoxide, acetone, and hexadecane) that would swell a conventional substrate for inkjet printing, polyethylene terephthalate (PET) and again found that only a small change in resistance occurred[34] (**Figure S4**).

To compare the performance conferred by different substrates to high-conductivity features, we printed wires (25 cm long, and 120 μm wide, printed with 5

layers of ink) of silver nanoparticle-, reactive silver-,[30] and carbon-based inks onto a series of "alkylated papers" ("R^H paper" produced by vapor-phase silanization of paper with alkyl trichlorosilanes), "fluoroalkylated papers" ("R^H paper" produced by vapor-phase silanization of paper with fluoroalkyl trichlorosilanes), and PET films, and tested their resistance. When using the same ink, wires printed on C_{10}^F and C_1^H treated paper have resistances comparable to wires printed on a commercial PET film designed for conductive inkjet printing (See **Table 1**).

To investigate the mechanical flexibility and resistance to creasing of the printed silver features, we produced a linear array (n=7) of them with width = 1 mm, and length = 10 cm, spaced 3 mm apart, using a single layer of reactive silver ink on Canson C_{10}^F-treated tracing paper. We measured the resistance of a feature as a function of the number of times we creased the sheet of paper on which they were printed. One cycle constituted folding the paper to a full crease –corresponding to the formation of a -180° angle (acute folding, silver on the inside) or a +180° angle (obtuse folding, silver on the outside) –and back. The ends of the electrode-patterned paper substrates were affixed to the crossheads of an Instron 5544A electromechanical testing machine, and the distance between the crossheads was cycled between 0 and 40 mm. Images of these samples undergoing a creasing cycle are shown in **Figure S5A-C**. A crosshead distance of 0 mm leads to the formation of a crease in the paper substrate in the direction perpendicular to the printed silver resistors. **Figure S5D** shows the averaged resistance values obtained from the array as a function of the number of creasing cycles. The resistance of the features did not vary significantly (<5%) from the original, pre-creasing resistance, after being folded to either a +180° or a -180° angle. This observation remained true for 100 consecutive folds; we

Table 1: Comparison between resistances (Ω) of wires [a)] (*n*=10) printed on different substrates—modified papers (C_1^H and C_{10}^F) and a PET film—using three different inks.

Ink tested	$R^{C_1^H}$ [Ω]	$R^{C_{10}^F}$ [Ω]	R^{PET} [Ω] [e)]
Reactive Silver Ink [b)]	5 ± 1	4 ± 1	13 ± 1
Silver Nano-particle Ink [c)]	24 ± 3	10 ± 4	33 ± 7
Carbon Ink (x10^{-4}) [d)]	87 ± 1	76 ± 2	65 ± 7

[a)] 25 cm x 120 μm wires were printed in 5 layers; [b)] Reactive Ag Ink #1 (Electroninks Inc.), [c)] Nanoparticle Colloidal Silver Ink DGP 40-LT-15C (Advanced Nano Products), [d)] Carbon Ink 3801 (Methode Electronics Ink); [e)] PET film (DuPont Melinex ST506/500).

observed no significant increase (<5 %) in the respective electrical resistance of the prints relative to their initial pre-creased values.

Electroadhesion. As a demonstration of the ability to print defect-free high-resolution conductive features over large areas, we prototyped flexible electroadhesive devices on omniphobic R^F tracing paper, using inkjet printing. Electroadhesion[35] is an electrically controlled adhesion technology used for applications that require reversible, adhesive-free, binding to a substrate.[36-41] A typical electroadhesion pad consists of two interdigitated electrodes patterned on the surface of a dielectric material. Electrostatic forces are created between electroadhesive pads and a substrate that is either electrically insulating or conductive (although much lower forces are achieved with electroadhesion for nonconducting objects).[38] Charging the interdigitated electrode creates fringe field lines between the positive and negative electrodes that extend in the direction normal to the electrode pattern. When the electroadhesive pad is brought in proximity to a substrate (e.g. glass, drywall, wood, concrete, metals), its fringe-field lines penetrate the substrate, and redistribute charge to create a pattern of opposite polarity in the substrate. [35-38] The coulombic attraction between the charges on the electrode and the complementary, induced charges on the surface of the substrate creates an electrostatic force that can be used to adhere the electroadhesive pad to the substrate. Controlling of the electrostatic adhesion voltage permits the adhesion to be turned on and off easily.

We used inkjet printing of the reactive silver ink to deposit a pair of interdigitated electrodes on a flexible dielectric layer (C_{10}^F-treated Canson tracing paper), in order to fabricate an electroadhesive device (**Figure 2**). The high resolution of the printing in conjunction with the use of omniphobic paper allowed us to deposit 500-μm wide

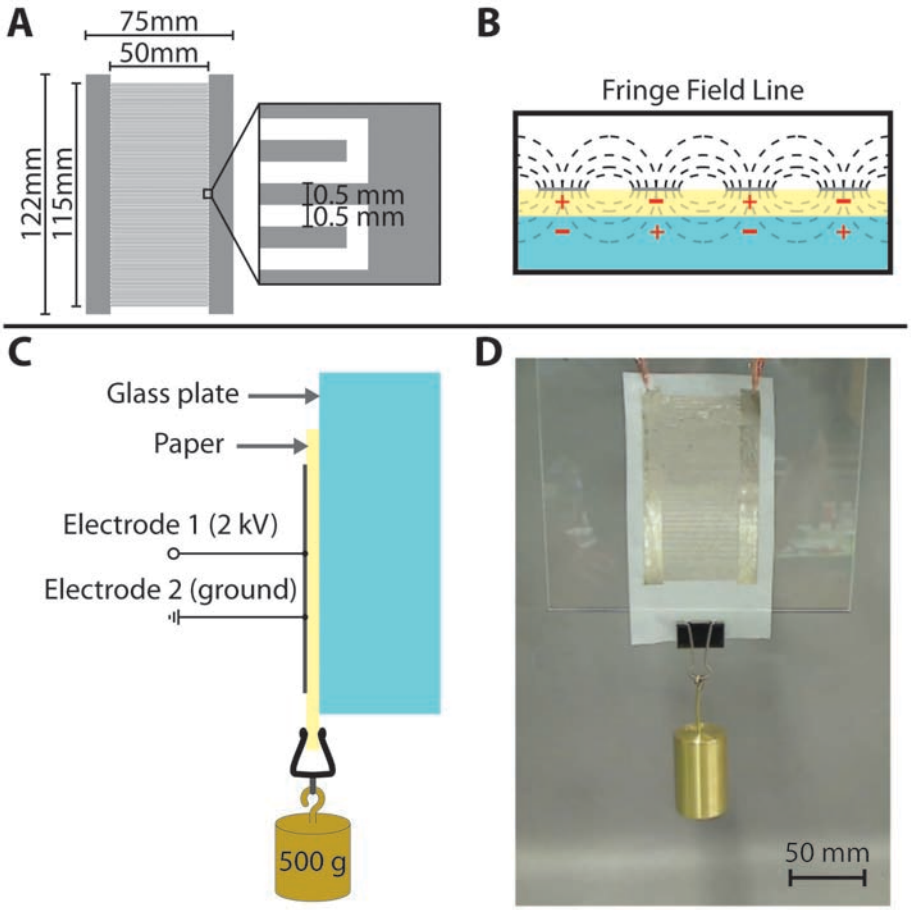

Figure 2: Silver electroadhesive pad printed on C_{10}^{F} Canson tracing paper using the reactive silver ink. **(A)** Schematic of the interdigitated electrode design used for the pad. **(B)** Illustration of a cross-section of the electroadhesive pad depicting the fringe electric field lines, generated from the electrode, charging a glass surface by induction. **(C)** Schematic showing the arrangement of the electroadhesive pad used for the experiment. **(D)** An electroadhesive pad (with dimensions given in A) under an applied 2 kV potential adheres to a glass plate with sufficient strength to support a 500g weight.

interdigitated electrodes over a large area (57.5 cm^2). This high resolution of printing resulted in a pattern that was free of defects that can cause short circuits; such short circuits, if present, would render the device inoperable. If the same pattern were printed using an inkjet printer and reactive silver ink on untreated paper, the bleeding of features into one another would cause short circuits. We applied a potential difference of 2 kV by connecting the electrodes to a high voltage power supply, and subsequently observed adhesion of the device to a glass surface that was sufficient to support a 500-g weight hanging from the base of the sheet (**Video M1**).

To demonstrate the utility of omniphobic R^F paper as a substrate for creating printed electronics, we fabricated mechanical and chemical sensors with carbon ink on C_{10}^F modified paper. We used carbon ink for the demonstration of paper-based MEMS and electrochemical devices in order to achieve a larger resistivity and a broader electrochemical window, respectively, than possible with silver inks. MEMS deflection sensors were fabricated to demonstrate an application in flexible electronics; electrochemical testing strips demonstrated an application that requires solvent-resistant electronics.

Paper MEMS. We fabricated cantilever-type MEMS deflection sensors by depositing carbon ink (Methode 3801) on C_{10}^F-treated Canson Vellum paper. Canson Vellum paper (Model No. 702-442) was used as a substrate for the printing of MEMS cantilever deflection sensors because it had a higher bending elastic modulus than many other papers. We tested the ability of a series (n=5) of these sensors (**Figure 3A** - Left) to measure beam deflection by cycling the device between an upward and downward deflection point while measuring the end-to-end resistance of the printed cantilever. An

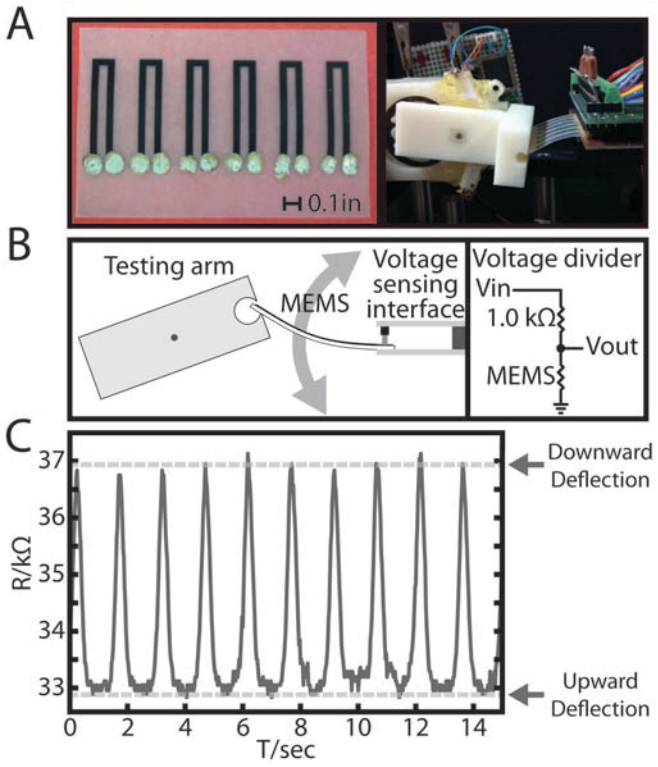

Figure 3: (A) Left, MEMS deflection sensor fabricated by depositing carbon ink on C_{10}^{F} Canson Vellum paper with an inkjet printer. Ercon 3456 silver ink was applied manually at the ends of the device to improve electrical connections with the testing rig. **Right,** Image of the experimental setup used for cyclically deflecting an array (*n*=5) of MEMS sensors. **(B)** Schematic describing the experimental setup (**Left**) and a diagram of the circuit employed for measuring device resistances (**Right**). **(C)** Plot of resistance vs. time for a representative device during 10 cycles of upward/downward deflection.

image and a schematic of the testing rig are shown in **Figure 3A** (right) and **3B** respectively. The plot in **Figure 3C** shows the resistance as a function of time of a typical device, as it is deflected cyclically. We observed a drop in resistance upon compression of the ink during upward deflection, reflecting (we hypothesize) an increase in the number of connections in the percolation network between carbon particles. A rise in resistance is observed during downward deflection as a result of a corresponding decrease in the number of connections upon extension.

Paper-Based Electrodes. We used inkjet printing to deposit arrays of electrodes over a non-planar paper surface consisting of wells embossed in omniphobic C_{10}^{F} paper. Whatman #1 Chromatography Paper is used as a substrate for the printing of electrochemical testing strips, because its high surface roughness increased the surface area accessible for electrochemical reactions and (in some applications) the sensitivity of detection. The electrode configuration consists of inkjet-printed working, counter, and quasi-reference carbon electrodes (WE, CE, and QRE, respectively). A well-defined area for the electrolyte/analyte solution is formed by partially overlapping the electrode area over an embossed well (**Figure 4A-D**). The electrochemical operation of the paper-based three-electrode system is tested by recording cyclic voltammograms for 1 mM and 100 μM solutions of 4-amino-phenol[42] (**Figure 4E**). The precise control over the positioning and volume of the droplets afforded by inkjet printing enabled us to print electrodes with a coefficient of variation as low as 2.1%, measured as the relative standard deviation (RSD, defined as the percentage ratio of the standard deviation to the mean of the distribution) in the peak anodic current (i_p, measured from the decaying cathodic current as a baseline,[43]) among different devices.

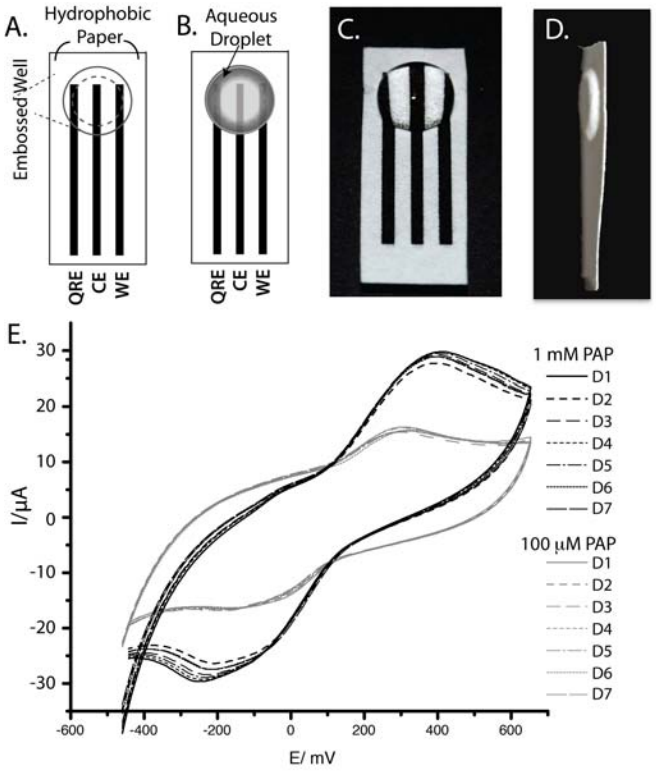

Figure 4: The reproducibility of electrodes, printed on embossed omniphobic C_{10}^{F} Whatman paper using carbon ink, as characterized by cyclic voltammetry. **(A)** Design of an electroanalytical device with a three-electrode system. The dotted line indicates that the embossed well is recessed into the surface and protrudes on the back side of the paper. **(B)** Illustration of the electroanalytical device with a drop placed in the embossed well. **(C)** Top view of an actual device with a 50-µL drop of an aqueous solution of an electroactive species added to the well. **(D)** Side-view. **(E)** Cyclic voltammograms of 4-aminophenol (PAP) at concentrations of 1 mM (black) and 100 µM (grey) tested on seven different devices (D1-D7). Potential measured vs. the quasi-reference electrode. Scan rate, 100 mV/s.

In summary, this paper describes the use of the inkjet printing to fabricate simple, flexible electronic devices on omniphobic R^F paper. These structures are thin, lightweight, breathable (permeable to gases) and resistant to damage by exposure to water and other common solvents. Unlike electronic systems fabricated on silicon, glass, ceramics or polymers, these structures can be folded and unfolded repeatedly, for storage in small spaces or to form three dimensional structures, and can be trimmed or shaped using scissors. The fact that electronics printed on R^F paper can be disposed of by incineration can help reduce environmental issues associated with the storage and management of electronic waste (end-of-life electronics). Our paper-based fabrication method has the potential to reduce the cost of development of electrical, electroanalytical and MEMS devices. In addition to use in health monitoring and diagnostics solutions in the developing world, low-cost, high- performance electronics may find commercial applications in economies in which cost is critically important.

Acknowledgments

Collaborative aspects of this work (JAL and GMW) were supported by the NSF Materials Research and Engineering Center (award DMR-0820484). Other work (GMW) was funded in part by the Bill & Melinda Gates Foundation (award # 51308) and (JAL) the Office of Naval Research through the Multi-University Research Initiative (MURI award N00014-11-1-0690). WowWee Group Limited (Hong Kong) assisted in the construction of the MEMS cyclic fatigue testing device. S.B. Walker gratefully acknowledges support through an IC Postdoctoral Fellowship. Supporting information is available online from Wiley InterScience or from the website of the Whitesides group (http://gmwgroup.harvard.edu/pubs).

References

[1] A. C. Glavan, R. V. Martinez, A. B. Subramaniam, H. J. Yoon, R. M. D. Nunes, H. Lange, M. M. Thuo, G. M. Whitesides., *Adv. Funct. Mater.* **2013** DOI: 10.1002/adfm.201300780.

[2] W. S. Bacon, *Pop Science* **1968**, *193*, 124.

[3] T. P. Brody, *IEEE Trans. Electron Devices* **1984**, *31*, 1614.

[4] A. C. Siegel, S. T. Phillips, M. D. Dickey, N. Lu, Z. Suo, G. M. Whitesides, *Adv. Funct. Mater.* **2010**, *20*, 28.

[5] R. Martins, I. Ferreira, E. Fortunato, *Phys. Status Solidi RRL* **2011**, *5*, 332.

[6] L. Hu, H. Wu, F. La Mantia, Y. Yang, Y. Cui, *ACS Nano* **2010**, *4*, 5843.

[7] D.-H. Kim, Y.-S. Kim, J. Wu, Z. Liu, J. Song, H.-S. Kim, Y. Y. Huang, K.-C. Hwang, J. A. Rogers, *Adv. Mater.* **2009**, *21*, 3703.

[8] U. Zschieschang, T. Yamamoto, K. Takimiya, H. Kuwabara, M. Ikeda, T. Sekitani, T. Someya, H. Klauk, *Adv. Mater.* **2011**, *23*, 654.

[9] M. C. Barr, J. A. Rowehl, R. R. Lunt, J. Xu, A. Wang, C. M. Boyce, S. G. Im, V. Bulović, K. K. Gleason, *Adv. Mater.* **2011**, *23*, 3500.

[10] D. Tobjork, R. Osterbacka, *Adv. Mater.* **2011**, *23*, 1935.

[11] G. Chinga-Carrasco, D. Tobjork, R. Osterbacka, *J. Nanopart. Res.* **2012**, *14*.

[12] F. Eder, H. Klauk, M. Halik, U. Zschieschang, G. Schmid, C. Dehm, *Appl. Phys. Lett.* **2004**, *84*, 2673.

[13] A. Russo, B. Y. Ahn, J. J. Adams, E. B. Duoss, J. T. Bernhard, J. A. Lewis, *Adv. Mater.* **2011**, *23*, 3426.

[14] A. W. Martinez, *Bioanalysis* **2011**, *3*, 2589.

[15] A. W. Martinez, S. T. Phillips, M. J. Butte, G. M. Whitesides, *Angew. Chem.* **2007**, *46*, 1318.

[16] A. W. Martinez, S. T. Phillips, E. Carrilho, S. W. Thomas, H. Sindi, G. M. Whitesides, *Anal. Chem.* **2008**, *80*, 3699.

[17] A. W. Martinez, S. T. Phillips, Z. Nie, C. M. Cheng, E. Carrilho, B. J. Wiley, G. M. Whitesides, *Lab Chip* **2010**, *10*, 2499.

[18] A. W. Martinez, S. T. Phillips, G. M. Whitesides, *Proc. Natl. Acad. Sci. U. S. A.* **2008**, *105*, 19606.

[19] A. W. Martinez, S. T. Phillips, G. M. Whitesides, E. Carrilho, *Anal. Chem.* **2010**, *82*, 3.

[20] A. W. Martinez, S. T. Phillips, B. J. Wiley, M. Gupta, G. M. Whitesides, *Lab Chip* **2008**, *8*, 2146.

[21] E. Carrilho, S. T. Phillips, S. J. Vella, A. W. Martinez, G. M. Whitesides, *Anal. Chem.* **2009**, *81*, 5990.

[22] S. A. Klasner, A. K. Price, K. W. Hoeman, R. S. Wilson, K. J. Bell, C. T. Culbertson, *Anal. Bioanal. Chem.* **2010**, *397*, 1821.

[23] E. Fu, P. Kauffman, B. Lutz, P. Yager, *Sens. Actuators, B* **2010**, *149*, 325.

[24] L. Ge, S. M. Wang, X. R. Song, S. G. Ge, J. H. Yu, *Lab Chip* **2012**, *12*, 3150.

[25] H. Liu, X. Li, R. M. Crooks, *Anal. Chem.* **2013**, *85*, 4263.

[26] K. Scida, B. L. Li, A. D. Ellington, R. M. Crooks, *Anal. Chem.* **2013**, *85*, 9713.

[27] T. Sekitani, Y. Noguchi, U. Zschieschang, H. Klauk, T. Someya, *Proc. Natl. Acad. Sci. U. S. A.* **2008**, *105*, 4976.

[28] C. W. Sele, T. von Werne, R. H. Friend, H. Sirringhaus, *Adv. Mater.* **2005**, *17*, 997.

[29] M. Singh, H. M. Haverinen, P. Dhagat, G. E. Jabbour, *Adv. Mater.* **2010**, *22*, 673.

[30] S. B. Walker, J. A. Lewis, *J. Am. Chem. Soc.* **2012**, *134*, 1419.

[31] A. W. Adamson, A. P. U. Gast, *Physical Chemistry of Surfaces*, Wiley, **1997**.

[32] I. Siro, D. Plackett, *Cellulose* **2010**, *17*, 459.

[33] S. H. Ko, H. Pan, C. P. Grigoropoulos, J. M. J. Frechet, C. K. Luscombe, D. Poulikakos, *Appl. Phys. A: Mater. Sci. Process.* **2008**, *92*, 579.
[34] PlasticsEurope, in *General Chemical Resistance of PET Products, retrieved at:* http://www.plasticseurope.org/Documents/Document/20100301162055-050303GeneralChemicalResistanceofPET-20050303-003-EN-v1.pdf 2010.
[35] G.J. Monkman, P.M. Taylor, G. J. Farnworth, *Int. J. Cloth. Sci. Tech.* **1989**, *1*, 14.
[36] G. Monkman, *Ind. Robot* **2003**, *30*, 326.
[37] G. J. Monkman, *Robotica* **1992**, *10*, 183.
[38] G. J. Monkman, *Int. J. Robot. Res.* **1997**, *16*, 1.
[39] H. Prahlad, R. Pelrine, S. Stanford, J. Marlow, R. Kornbluh, *IEEE Int. Conf. Robot. Autom.* **2008**, *1-9*, 3028.
[40] H. Prashad, *Trans. ASME. J. Tribol.* **1988**, *110*, 448.
[41] H. Q. Wang, A. Yamamoto, T. Higuchi, *IEEE Int. Conf. Robotic. Autom.* **2012**, 914.
[42] O. Niwa, Y. Xu, H. B. Halsall, W. R. Heineman, *Anal. Chem.* **1993**, *65*, 1559.
[43] A. J. Bard, L. R. Faulkner, *Electrochemical Methods*, John Wiley & Sons, New York **2001**.

Supporting Information

Inkjet Printing of Conductive Inks with High Lateral Resolution on Omniphobic "R^F Paper" for Paper-Based Electronics and MEMS.

Joshua Lessing[1], Ana C. Glavan[1], S. Brett Walker[2,3], Christoph Keplinger[1], Jennifer A. Lewis[2,3,] and George M. Whitesides[1,2,*]*

[* corresponding authors] Prof. J. A. Lewis and Prof. G. M. Whitesides
E-mail: jalewis@seas.harvard.edu and gwhitesides@gmwgroup.harvard.edu

[1] Department of Chemistry and Chemical Biology, Harvard University, 12 Oxford Street, Cambridge, MA 02138, (USA).
[2] Wyss Institute for Biologically Inspired Engineering, Harvard University, 3 Blackfan Circle, Boston, MA 02115, (USA)
[3]Harvard School of Engineering and Applied Sciences, 29 Oxford Street, Cambridge, MA 02138, (USA).

Experimental

Fabrication of R^H and R^F papers. The silanizing reagents: tris(dimethylamino)silane (TDAS), tricholoromethylsilane (CH_3SiCl_3, "C_1^H"), trichlorodecylsilane ($CH_3(CH_2)_9SiCl_3$, "C_{10}^H"), trichloro(3,3,4,4,5,5,6,6,7,7,8,8,9,9,10,10,10-heptadecafluorodecyl)silane ($CF_3(CF_2)_7CH_2$-CH_2SiCl_3, "C_{10}^F"), were purchased from Gelest Inc (Morrisville, PA). All chemicals were used as received without further purification. Canson tracing paper, Model No. 702-321, and Canson Vellum paper, Model No. 702-442 were purchased from Blick Art (Cambridge, MA, USA) and used as received. Whatman #1 Chromatography Paper was purchased from GE Healthcare (NJ, USA) and used as received.

The silanization reaction was conducted in a chamber with a volume of 0.01 m^3 at a temperature set at 105 °C. The silanizing reagent was transferred into a glass vial and placed inside the chamber together with the samples. Each experiment typically required ~100 mg of silane in 5 mL of anhydrous toluene. The silane was vaporized at 105 °C under reduced pressure (~30 mbar, ~0.03 atm) and allowed to react for 5 minutes. Diffusion inside the reaction chamber was sufficient for an even distribution of the silane within the chamber.

Inkjet printing: All inkjet printing was performed using a Fuji Dimatix DMP-2831 which dispensed inks using the Fuji Dimatix model waveform. Droplets were dispensed from a 10 pL cartridge; drop spacing was set at 20 μm and printing frequency at 5-10 kHz (except for the electroadhesive pad which used a 1 pL cartridge with a drop spacing of 9 μm). The Fuji Dimatix model waveform used an ejection voltage of 40V (except for the minimum wire resolution test that used an ejection voltage of 18-24V). The nozzles were heated to 30-33°C with a vacuum of 4 in H_2O for silver inks and 5 in H_2O for Methode 3801 carbon ink.

Characterization of the solvent resistance of printed conductive features on omniphobic R^F paper. Solvents were used as received: anhydrous ethanol (Pharmco-Aaper, 200 proof, absolute), *n*-hexadecane (Sigma-Aldrich, anhydrous, ≥99%), chloroform (Sigma-Aldrich, anhydrous, ≥99%), acetone (Sigma-Aldrich, anhydrous, ≥99%), acetic acid (Sigma-Aldrich, glacial), (DMSO (Sigma-Aldrich, anhydrous, ≥99%), glycerin (Sigma-Aldrich, anhydrous, ≥99%), toluene (Acros, spectrophotometric grade 99+%), dimethylsulfoxide (DMSO, Sigma-Aldrich, anhydrous 99.9%). Water is ultrapure and deionized (resistivity = 18.2 MΩ-cm).

In each solvent test, 10 distinct drops (volume = 50 μL) were added along the conductive path of each individual printed wire. The resistance of the wire was measured before the addition

of the drops, and 30 minutes after it, using the test leads of a digital multimeter. For each solvent, the procedure was repeated for seven distinct wires.

Contact angle measurements. The contact angle measurements were performed using a contact angle measurement system (Ramé-Hart model 500-F1, Ramé-Hart Instrument Co.) at room temperature (20 – 25 °C) with ~20% relative humidity. The droplet volume for the measurement was ~10 µL (unless otherwise specified). The droplet profile was fitted to a spherical profile using the software provided by the system (DROPimage Advanced, v. 2.0).

Polymeric films used as substrates for printing: The Melinex ST506/500 films were provided by DuPont Teijin Films.

Inkjet inks: The following inks were printed on Melinex ST506/500, C_1^H treated Canson tracing paper and C_{10}^F treated Canson tracing paper to compare the resistance of different combinations of substrate and ink: DGP 40-LT-15C (Advanced Nano Products), reactive silver ink (Electroninks Inc.), and carbon ink 3801 (Methode Electronics Inc.).

Scanning electron microscopy: SEM data was collected on unmetalized samples using a Zeiss Ultra Plus FESEM with an Extra High Tension of 2kV and a working distance ranging from 8.9 mm-9.7 mm collected with a positively biased Everhart-Thornley detector.

Resistance measurements: The resistance of the wires was measured using the test leads of a digital multimeter.

MEMS. The MEMS pattern was printed in three passes. For the MEMS deflection sensor, we manually applied Ercon 3456 silver ink to the ends of each cantilever to improve electrical connections with the voltage sensing pins of the testing apparatus.

Theory of wetting. The wettability of the substrate dictates how well the inkjet printed fluids will wet and spread. The spreading parameter (Equation 1), where γ_{SV}, γ_{LV}, and γ_{SL} are the solid–vapor, liquid–vapor, and solid–liquid surface energies per unit area, respectively, describes the thermodynamic criterion for equilibrium wetting of chemically homogenous smooth solid substrates. When $S \geq 0$, the process is accompanied by a decrease in free energy and the liquid displaces the vapor phase, wetting the substrate completely; when $S < 0$, the liquid forms a drop with a definite angle of contact between the liquid phase and the solid substrate. [1]

$$S = \gamma_{SV} - (\gamma_{LV} + \gamma_{SL}) \quad (1)$$

The interfacial interaction leading to the formation of a drop on the surface is described by Young´s equation (Equation 2): [1]

$$cos\,\theta_s = \frac{\gamma_{SV} - \gamma_{SL}}{\gamma_{LV}} \quad (2)$$

[1] A. W. Adamson, A. P. U. Gast, *Physical Chemistry of Surfaces*, Wiley, 1997.

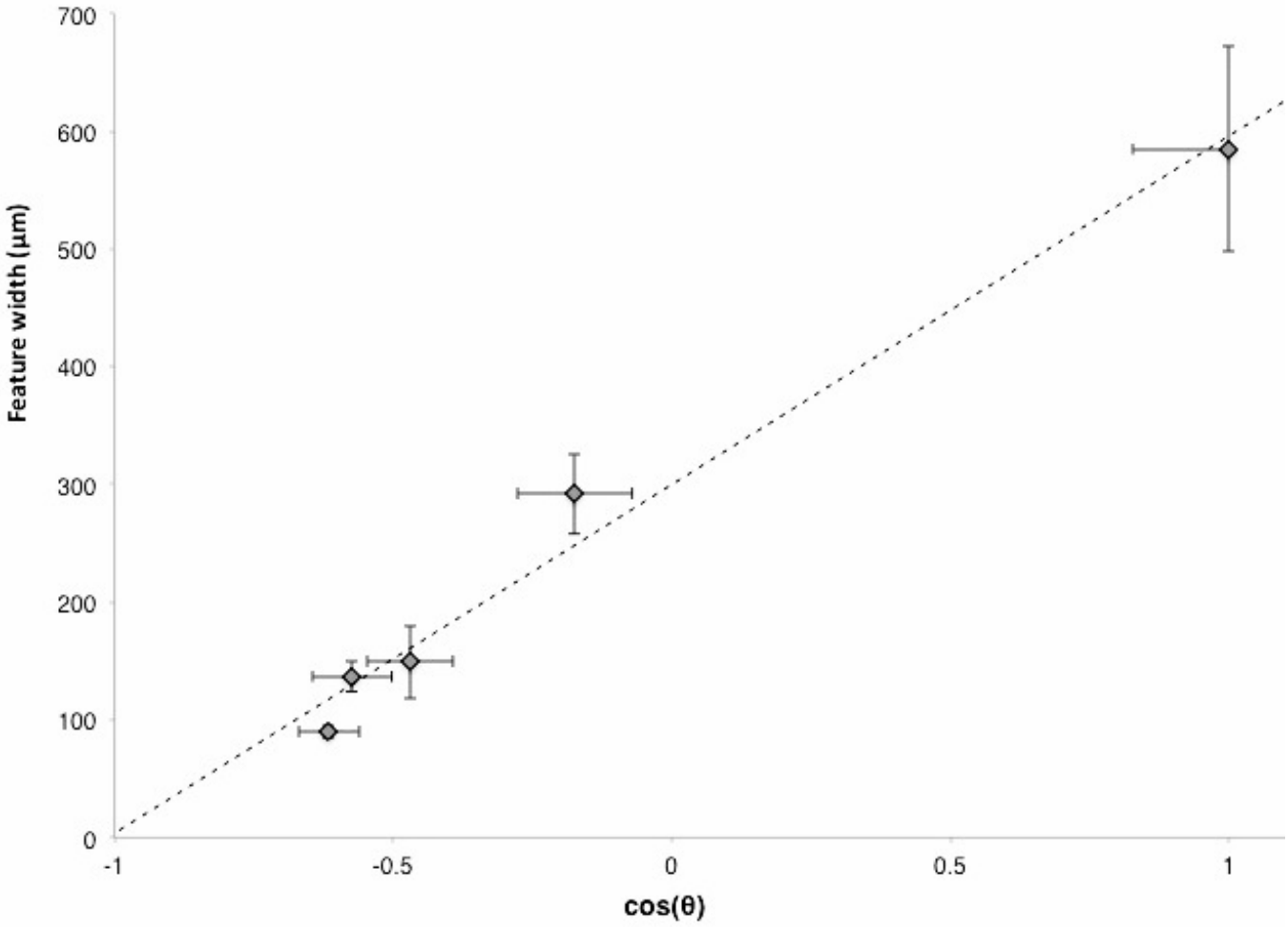

Figure S1: Relationship between the width of features printed on a modified or unmodified paper, and the contact angle of water on the respective surface. The data is fitted to a linear trendline with the equation: $y = 296.12x + 299.9$, $R^2=0.98$.

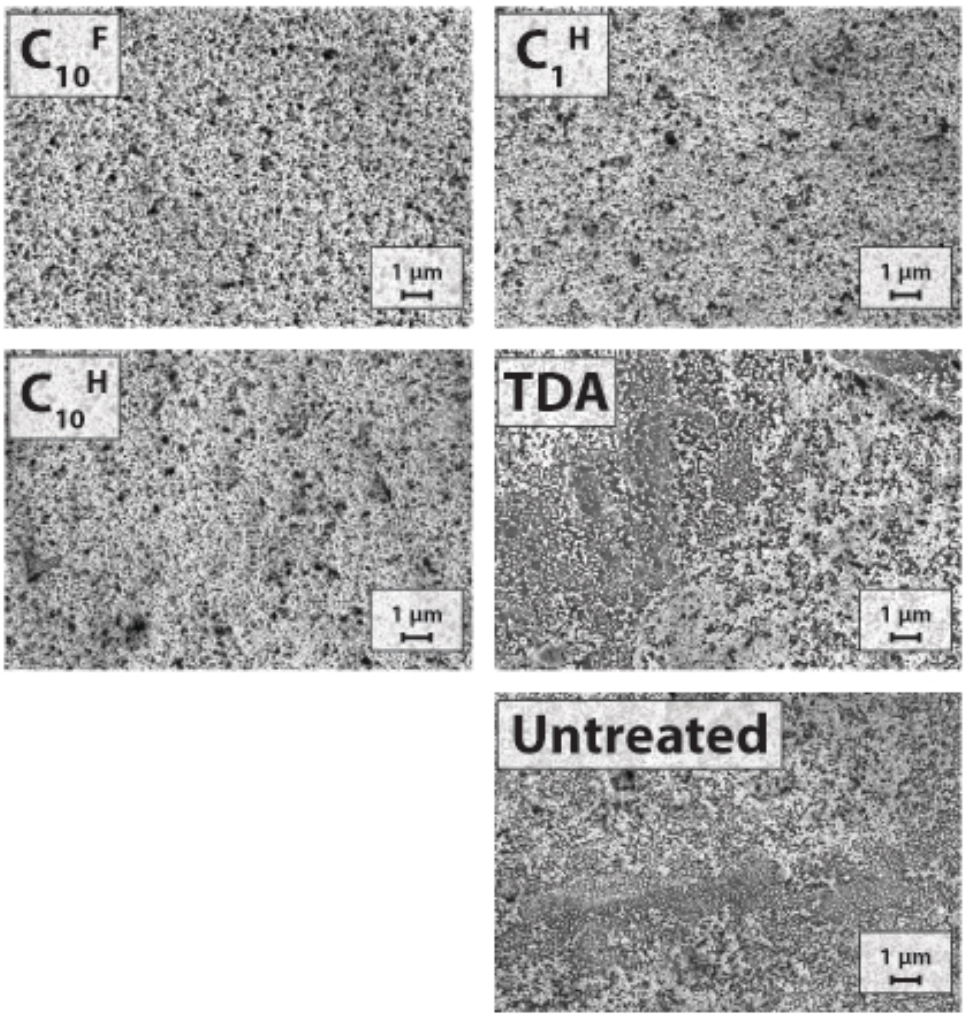

Figure S2. SEM images of reactive silver ink printed on treated and untreated papers.

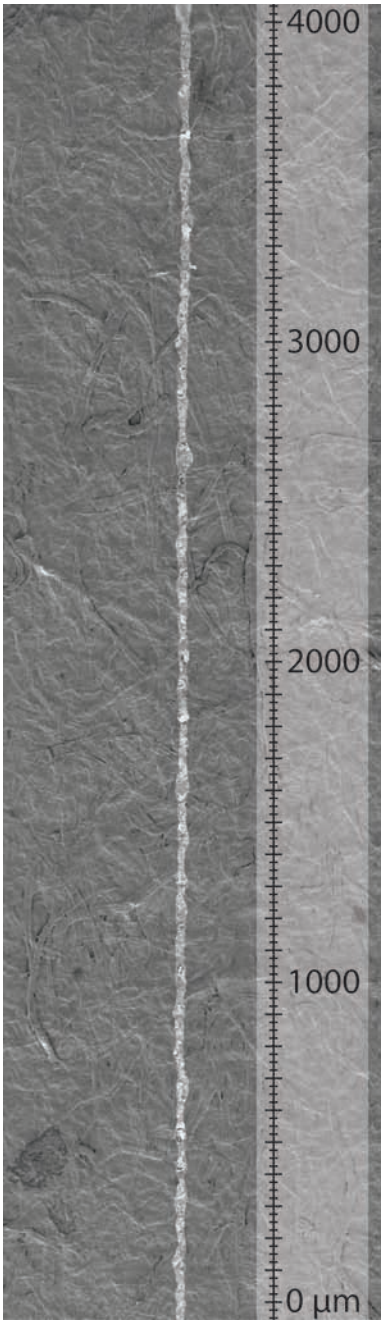

Figure S3: SEM image of a 4 mm-long silver feature printed using 10 pL droplets of reactive silver ink, with 20 µm spacing between drops, on C_{10}^{F}–treated Canson tracing paper. The feature depicted here has an average width of 28 ± 5 µm (*n*=41) and a line edge roughness of

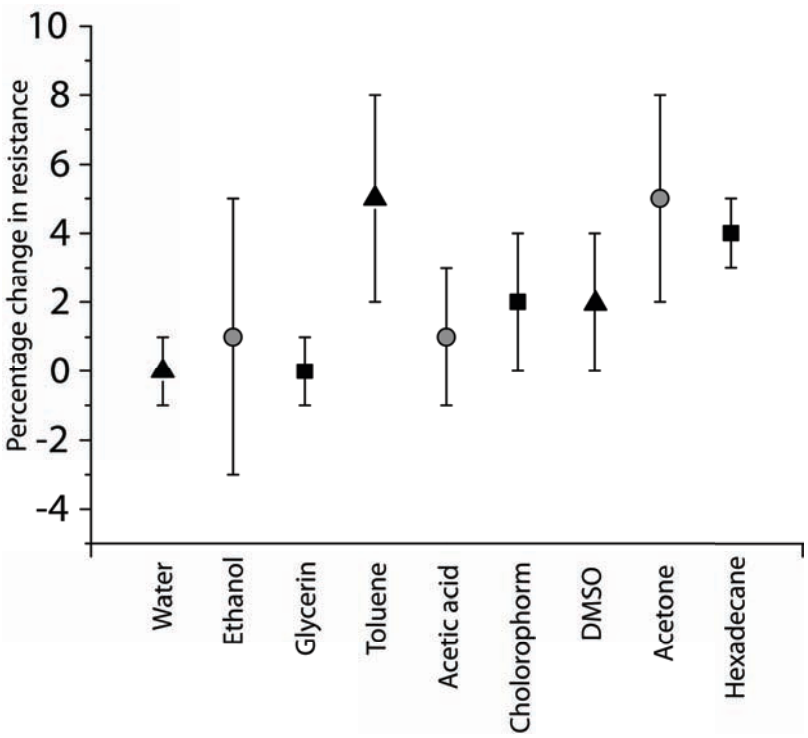

σ_{LER} = 6 μm (*n*=41).

Figure S4: Percentage change in resistance following exposure of wires printed on C_{10}^{F} omniphobic paper to solvent. Ten 50 μL drops of solvent were deposited along the path of each 1 mm wide, 10 cm-long wire (*n*=7 wires were tested per solvent) printed with reactive silver ink, and the end to end resistance was measured before and after solvent exposure.

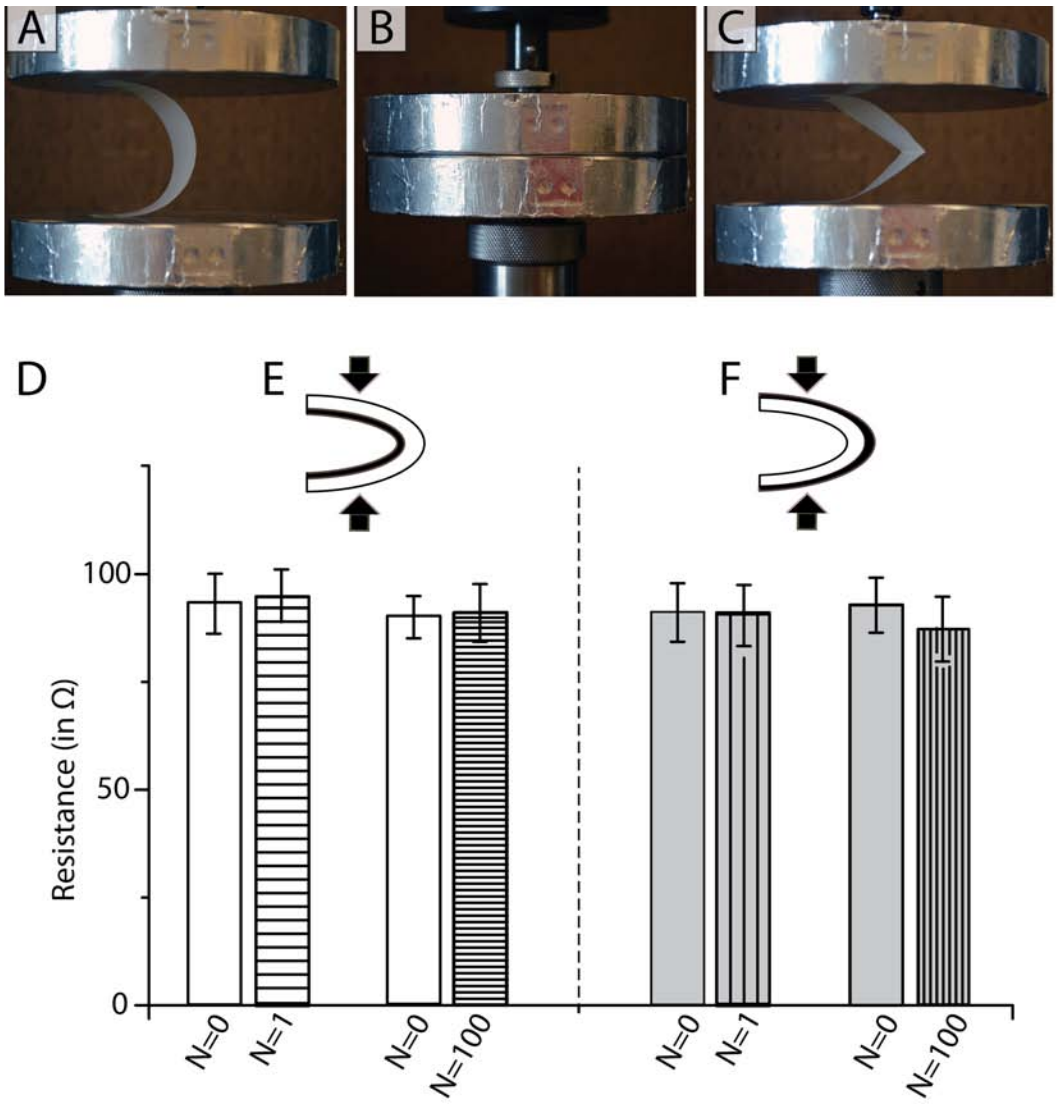

Figure S5: Resistance to creasing of printed conductive features: (A, B, C) Images of the test specimens undergoing a creasing cycle. (D) No significant increase in the respective electrical resistance was observed for the conductive prints relative to their initial, as-printed state, when the creasing occurs with the silver features either in (E) compression or in (F) extension.